

# High precision study for rho-meson resonance from Lattice QCD

Dehua Guo, Andrei Alexandru, Raquel Molina and Michael Döring

GWU Nuclear Seminar

March 1, 2016

Why we study resonance from Lattice QCD?

- Lattice QCD offers us a way to study the resonances in terms of quark and gluon dynamics. It serves as a test of QCD for well determined resonance parameters.
- The techniques can be used to investigate systems where the experimental situation is less clear.
- Validate effective models used to describe hadron scattering.

How?

- We start from meson resonance because they have better signal-to-noise ratio.
- $\rho(770)$  resonance in  $I = 1, J = 1$   $\pi$ - $\pi$  scattering channel.

## Symmetries on the lattice

On the lattice, the energy eigenstates  $|n\rangle$  of the system are computed in a given irrep of the lattice symmetry group.

$$\psi_n(R^{-1}x) = \psi_n(R^{-1}(x + \mathbf{n}L)); \quad \langle \hat{O}_2(t) \hat{O}_1^\dagger(0) \rangle = \sum_n \langle 0 | \hat{O}_2 | n \rangle \langle n | \hat{O}_1 | 0 \rangle e^{-tE_n} \quad (1)$$

Isospin, color and flavor symmetries are similar to the continuum.

Table : Irreducible representation in  $SO(3)$ ,  $O$  and  $D_4$

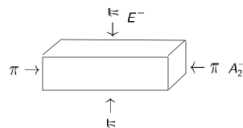
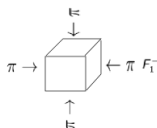
	$SO(3)$	cubic box( $O_h$ )	elongated box( $D_{4h}$ )
irep label	$Y_{lm}; l = 0, 1, \dots, \infty$	$A_1, A_2, E, F_1, F_2$	$A_1, A_2, E, B_1, B_2$
dim	$1, 3, \dots, 2l + 1, \dots, \infty$	$1, 1, 2, 3, 3$	$1, 1, 2, 2, 2$

Table : Angular momentum mixing among the irreducible representations of the lattice group

$O_h$		$D_{4h}$	
irreducible representation	$l$	irreducible representation	$l$
$A_1$	0, 4, 6, ...	$A_1$	0, 2, 3, ...
$A_2$	3, 6, ...	$A_2$	1, 3, 4, ...
$F_1$	1, 3, 4, 5, 6, ...	$B_1$	2, 3, 4, ...
$F_2$	2, 3, 4, 5, 6, ...	$B_2$	2, 3, 4, ...
$E$	2, 4, 5, 6, ...	$E$	1, 2, 3, 4, ...

# Symmetries of the elongated box

$\rho$  resonance is in  $I = 1, J^P = 1^-$  channel for pion-pion scattering. Elongated box method tunes the momentum of the scattering particles on the lattice  $\mathbf{p} \propto (\frac{2\pi}{\eta L})$ .



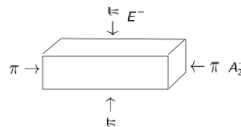
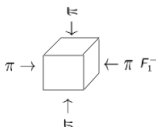
The  $SO(3)$  symmetry group reduce to discrete subgroup  $O_h$  or  $D_{4h}$

$J$	$O_h$	$D_{4h}$
0	$A_1^+$	$A_1^+$
1	$F_1^-$	$A_2^- \oplus E^-$
2	$E^+ \oplus F_2^+$	$A_1^+ \oplus B_1^+ \oplus B_2^+ \oplus E^+$
3	$A_2^- \oplus F_1^- \oplus F_2^-$	$A_2^- \oplus B_1^- \oplus B_2^- \oplus 2E^-$
4	$A_1^+ \oplus E^+ \oplus F_1^+ \oplus F_2^+$	$2A_1^+ \oplus A_2^+ \oplus B_1^+ \oplus B_2^+ \oplus 2E^+$

For the p-wave ( $I = 1$ ) scattering channel, we only need to construct the interpolating fields in  $F_1^-$  in the  $O_h$  group,  $A_2^-$  representations in  $D_{4h}$  group because the energy contribution from angular momenta  $I \geq 3$  is negligible.

# Lüscher's formula for elongated box [1]

Phase shift for  $l = 1$ , rest frame ( $\mathbf{P} = 0$ ):



$$A_2^- : \cot \delta_1(k) = \mathcal{W}_{00} + \frac{2}{\sqrt{5}} \mathcal{W}_{20} \quad (2)$$

$$(3)$$

$$\mathcal{W}_{lm}(1, q^2, \eta) = \frac{\mathcal{Z}_{lm}(1, q^2, \eta)}{\eta \pi^{\frac{3}{2}} q^{l+1}}; \quad q = \frac{kL}{2\pi}; \quad \eta = \frac{N_{el}}{N} : \text{elongation factor} \quad (4)$$

Zeta function

$$\mathcal{Z}_{lm}(s; q^2, \eta) = \sum_{\tilde{\mathbf{n}}} \mathcal{Y}_{lm}(\tilde{\mathbf{n}}) (\mathbf{n}^2 - q^2)^{-s}; \quad \mathbf{n} \in \mathbf{m} \quad (5)$$

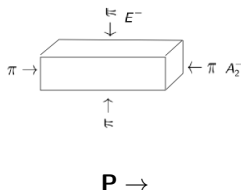
Total energy

$$E = 2\sqrt{m^2 + k^2}; \quad k = \sqrt{\left(\frac{E}{2}\right)^2 - m^2} \quad (6)$$

[1] X. Feng, X. Li, and C. Liu, Phys.Rev. D70 (2004) 014505

## Lüscher's formula for boost frame

In order to obtain new kinematic region, we boost the resonance along the elongated direction.



$$A_2^- : \cot \delta_1(k) = \mathcal{W}_{00} + \frac{2}{\sqrt{5}} \mathcal{W}_{20} \quad (7)$$

(8)

$$\mathcal{W}_{lm}(1, q^2, \eta) = \frac{\mathcal{Z}_{lm}^{\mathbf{P}}(1, q^2, \eta)}{\gamma \eta \pi^{\frac{3}{2}} q^{l+1}}; \quad \eta = \frac{N_{el}}{N} : \text{elongation factor}; \quad \gamma : \text{boost factor}; \quad (9)$$

$$\mathcal{Z}_{lm}^{\hat{\mathbf{P}}}(s; q^2, \eta) = \sum_{\mathbf{n}} \mathcal{Y}_{lm}(\tilde{\mathbf{n}})(\tilde{\mathbf{n}}^2 - q^2)^{-s}; \quad \mathbf{n} \in \frac{1}{\gamma}(\mathbf{m} + \frac{\hat{\mathbf{P}}}{2}); \quad (10)$$

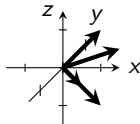
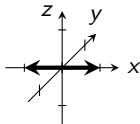
## Interpolating field construction for $\rho$ resonance

Four  $q\bar{q}$  operators and two scattering operators  $\pi\pi$  in  $A_2^-$  sector.

$$\rho^J(t_f) = \bar{u}(t_f)\Gamma_{t_f}A_{t_f}(\mathbf{p})d(t_f); \quad \rho^{J\dagger}(t_i) = \bar{d}(t_i)\Gamma_{t_i}^\dagger A_{t_i}^\dagger(\mathbf{p})u(t_i) \quad (11)$$

$N$	$\Gamma_{t_f}$	$A_{t_f}$	$\Gamma_{t_i}^\dagger$	$A_{t_i}^\dagger$
1	$\gamma_i$	$e^{i\mathbf{p}}$	$-\gamma_i$	$e^{-i\mathbf{p}}$
2	$\gamma_4\gamma_i$	$e^{i\mathbf{p}}$	$\gamma_4\gamma_i$	$e^{-i\mathbf{p}}$
3	$\gamma_i$	$\nabla_j e^{i\mathbf{p}} \nabla_j$	$\gamma_i$	$\nabla_j^\dagger e^{-i\mathbf{p}} \nabla_j^\dagger$
4	$\frac{1}{2}$	$\{e^{i\mathbf{p}}, \nabla_i\}$	$-\frac{1}{2}$	$\{e^{-i\mathbf{p}}, \nabla_i\}$

$$(\pi\pi)_{\mathbf{P},\Lambda,\mu} = \sum_{\mathbf{p}_1^*, \mathbf{p}_2^*} C(\mathbf{P}, \Lambda, \mu; \mathbf{p}_1; \mathbf{p}_2) \pi(\mathbf{p}_1) \pi(\mathbf{p}_2), \quad (12)$$



$$\pi\pi_{100}(\mathbf{p}_1, \mathbf{p}_2, t) = \frac{1}{\sqrt{2}} [\pi^+(\mathbf{p}_1)\pi^-(\mathbf{p}_2) - \pi^+(\mathbf{p}_2)\pi^-(\mathbf{p}_1)]; \quad \mathbf{p}_1 = (1, 0, 0) \quad \mathbf{p}_2 = (-1, 0, 0)$$

$$\pi\pi_{110} = \frac{1}{2} (\pi\pi(110) + \pi\pi(101) + \pi\pi(1-10) + \pi\pi(10-1))$$

## 6 × 6 correlation matrix

$$C = \begin{pmatrix} C_{\rho^J \leftarrow \rho^{J'}} & C_{\rho^J \leftarrow \pi \pi_{100}} & C_{\rho^J \leftarrow \pi \pi_{110}} \\ C_{\pi \pi_{100} \leftarrow \rho^{J'}} & C_{\pi \pi_{100} \leftarrow \pi \pi_{100}} & C_{\pi \pi_{100} \leftarrow \pi \pi_{110}} \\ C_{\pi \pi_{110} \leftarrow \rho^{J'}} & C_{\pi \pi_{110} \leftarrow \pi \pi_{100}} & C_{\pi \pi_{110} \leftarrow \pi \pi_{110}} \end{pmatrix}. \quad (13)$$

The correlation functions:  $\bar{u}(t_i) \longrightarrow u(t_f)$

$$C_{\rho_i \leftarrow \rho_j} = - \left\langle \begin{array}{c} \Gamma_{t_f}^J(\mathbf{p}, t_f) \\ \text{loop} \\ \Gamma_{t_i}^{J'\dagger}(-\mathbf{p}, t_i) \end{array} \right\rangle = - \left\langle \text{Tr}[M^{-1}(t_i, t_f) \Gamma_{t_f}^J e^{i\mathbf{p}} M^{-1}(t_f, t_i) \Gamma_{t_i}^{J'\dagger} e^{-i\mathbf{p}}] \right\rangle. \quad (14)$$

$$C_{\rho_i \leftarrow \pi \pi} = \left\langle \begin{array}{c} \text{triangle} \\ \text{triangle} \end{array} \right\rangle - \left\langle \begin{array}{c} \text{triangle} \\ \text{triangle} \end{array} \right\rangle \stackrel{\mathbf{P}=0}{=} 2 \left\langle \begin{array}{c} \text{triangle} \\ \text{triangle} \end{array} \right\rangle. \quad (15)$$

$$C_{\pi \pi \leftarrow \pi \pi} = - \left\langle \begin{array}{c} \text{square} \\ \text{square} \\ \text{X} \\ \text{X} \\ \text{figure-eight} \\ \text{loop} \end{array} \right\rangle \quad (16)$$

$$\stackrel{\mathbf{P}=0}{=} - \left\langle 2 \begin{array}{c} \text{square} \\ \text{X} \\ \text{figure-eight} \\ \text{loop} \end{array} \right\rangle \quad (17)$$



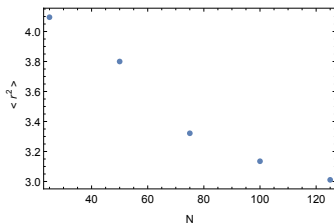
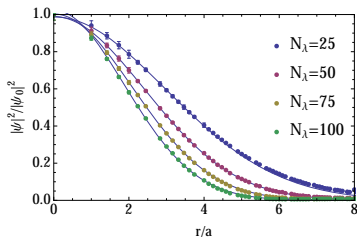
## Laplacian Heaviside smearing [2]

To estimate all-to-all propagators:  
The 3-dimensional gauge-covariant Laplacian operator



$$\tilde{\Delta}^{ab}(x, y; U) = \sum_{k=1}^3 \left\{ \tilde{U}_k^{ab}(x) \delta(y, x + \hat{k}) + \tilde{U}_k^{ba}(y)^* \delta(y, x - \hat{k}) - 2\delta(x, y) \delta^{ab} \right\}. \quad (18)$$

$$S_\Lambda(t) = \sum_{\lambda(t)}^\Lambda |\lambda(t)\rangle \langle \lambda(t)|; \quad \tilde{u}(t) = S(t)u(t) = \sum_{\lambda_t} |\lambda_t\rangle \langle \lambda_t| u(t). \quad (19)$$



[2] C. Morningstar, J. Bulava, J. Foley, K. J. Juge, D. Lenkner, et al., Phys.Rev. D83 (2011) 114505

## $\rho$ energy spectrum

We implement the calculation in 3 ensembles ( $\eta = 1.0, 1.25, 2.0$ ) at  $m_\pi \approx 310$  MeV and 3 ensembles ( $\eta = 1.0, 1.17, 1.33$ ) at  $m_\pi \approx 227$  MeV with nHYP-smeared clover fermions and two mass-degenerated quark flavor.

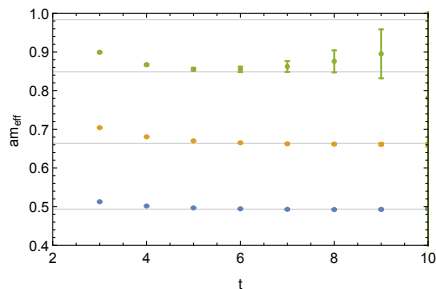
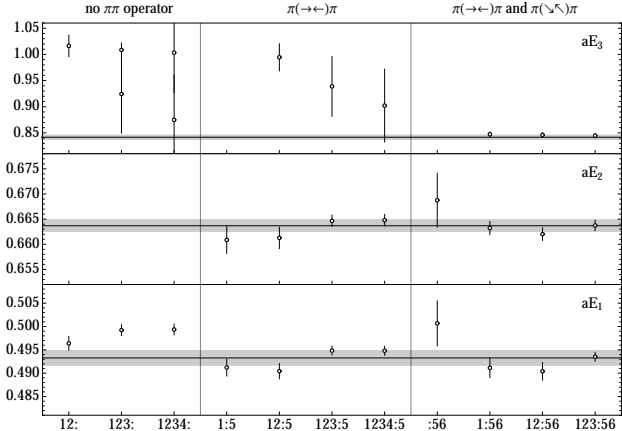


Figure : The lowest three energy states with their error bars for  $\eta = 1.0, m_\pi = 310$  MeV ensemble

We extract energy  $E$  by using double exponential  $f(t) = we^{-Et} + (1 - w)e^{-E't}$  to do the  $\chi^2$  fitting for each eigenvalues.

# Energy spectrum



$\mathcal{O}_i$	1	2	3	4	5	6
	$\rho_1$	$\rho_2$	$\rho_3$	$\rho_4$	$\pi\pi_{100}$	$\pi\pi_{110}$

(20)

# Expectation for energy states

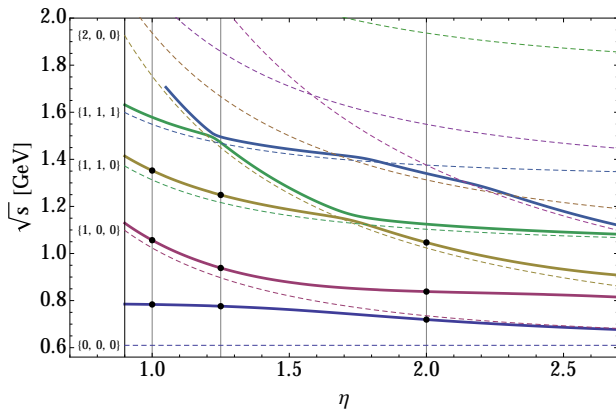
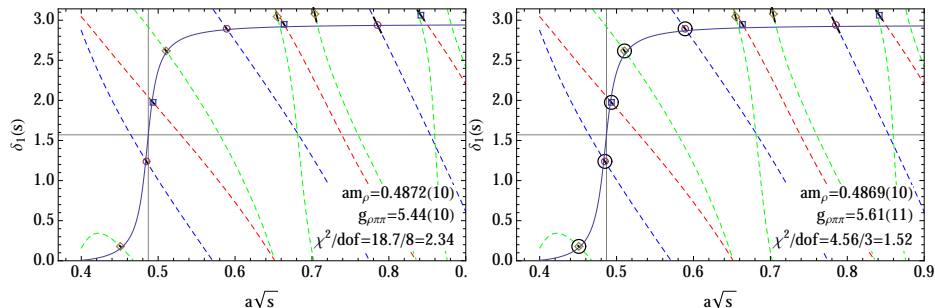


**Figure :** The lowest 3 energy states prediction from unitary  $\chi$ PT. When  $\eta = 2.0$  the 3rd state is from operator  $\pi\pi_{200}$  instead of  $\pi\pi_{110}$

## Phase shifts and resonance parameters

**Figure :** Phaseshift data from three ensembles fitted with Breit Wigner form (left) and only fit 5 data points in the resonance region .



$$\cot(\delta_1(E)) = \frac{M_R^2 - E^2}{E\Gamma_r(E)} \text{ where } \Gamma_r(E) \equiv \frac{g_{R12}^2}{6\pi} \frac{p^3}{E^2}. \quad (21)$$

$$\delta_1(E) = \arccot \frac{6\pi(M_R^2 - E^2)E}{g^2 p^3} \quad (22)$$

## Centrifugal barrier term [3]

Based on the idea that resonance has finite spatial size,  $\Gamma_r$  is expected to be damped faster than Breit Wigner form above the resonance region. Modify BW with a centrifugal barrier term.

$$\Gamma_r(E) = \frac{g^2}{6\pi} \frac{p^3}{E^2} \frac{1 + (p_R R)^2}{1 + (pR)^2}. \quad (23)$$

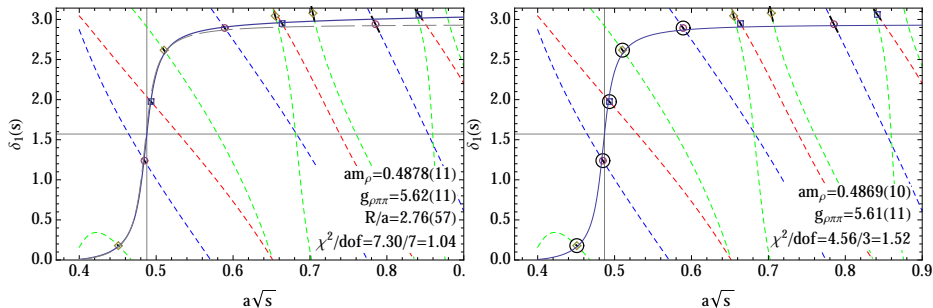
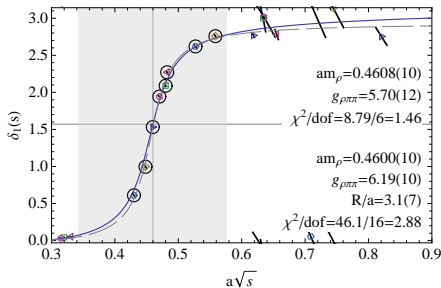
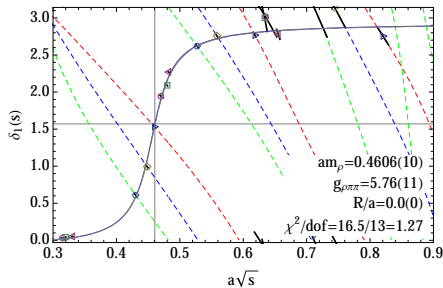
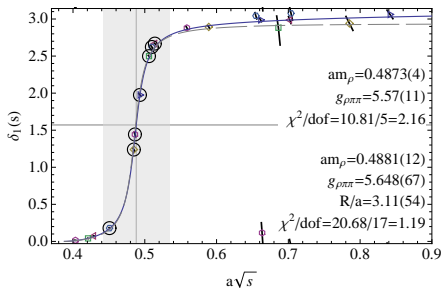
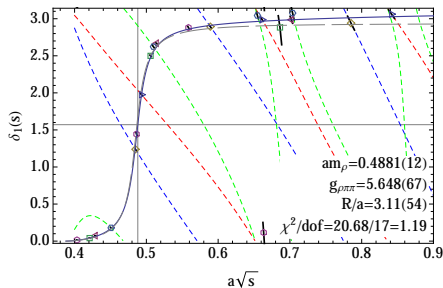


Figure : (left) Current study with LapH smearing vs (right) fitting only the resonance region

[3] F. Von Hippel and C. Quigg, Phys.Rev. D5 (1972) 624-638.

# Fit in $m_\rho \pm 2\Gamma$ with BW



## Fit with other models

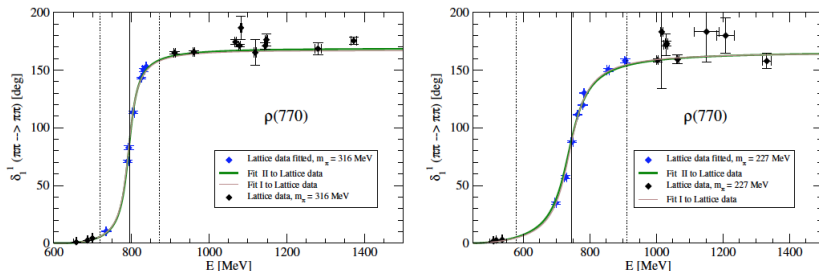


Figure : Two pion mass lattice data fitted with  $U\chi PT$  model in  $m_\rho \pm 2\Gamma$  region.

	$m_\pi$	$m_\rho$	$\Gamma_\rho$	$g$	$\chi^2/dof$
Breit Wigner	315	794.6(6)	37.0(2)	5.57(11)	2.16
$U\chi PT$		795.2(3)	36.1(1)		1.26
Breit Wigner	227	748.4(1.6)	71.0(8)	5.70(12)	1.46
$U\chi PT$		748.2(7)	77.0(5)		1.53



## $m_\rho$ and $g_{\rho\pi\pi}$ comparison

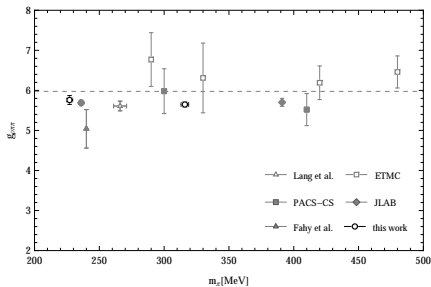
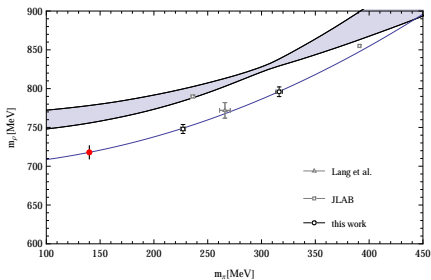


Figure :  $m_\pi^2$  extrapolation to physical pion mass

The extrapolation value of  $m_\rho$  at physical pion mass is  $715(7) \text{ MeV} < m_\rho = 775 \text{ MeV}$ .

## $K\bar{K}$ channel contribution

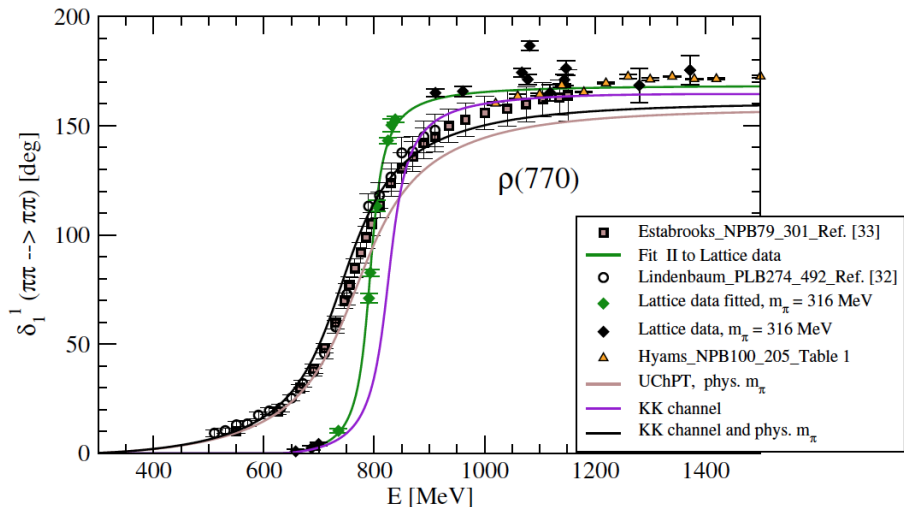


Figure :  $m_\pi = 315$  MeV data fitted with Unitary  $\chi$ PT model and their  $K\bar{K}$  channel corrections

## $K\bar{K}$ channel contribution

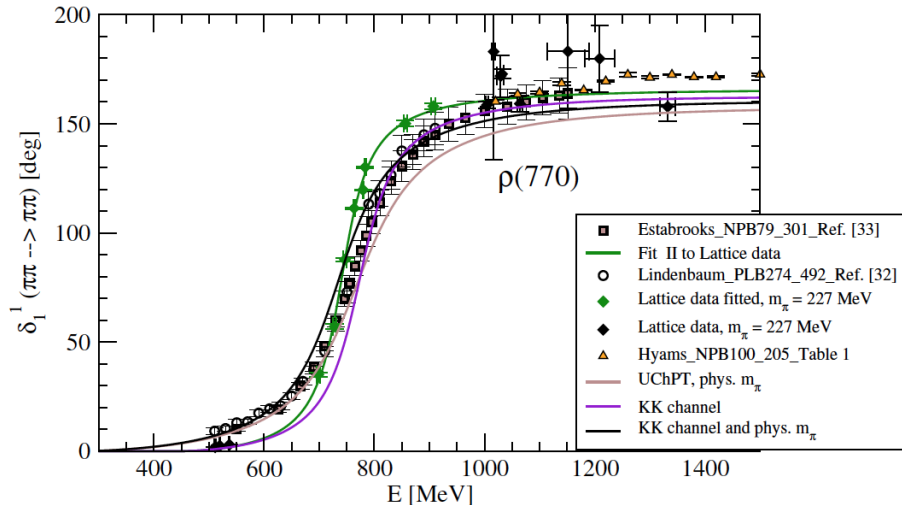


Figure :  $m_\pi = 227$  MeV data fitted with Unitary  $\chi$ PT model and their  $K\bar{K}$  channel corrections

## $K\bar{K}$ channel contribution

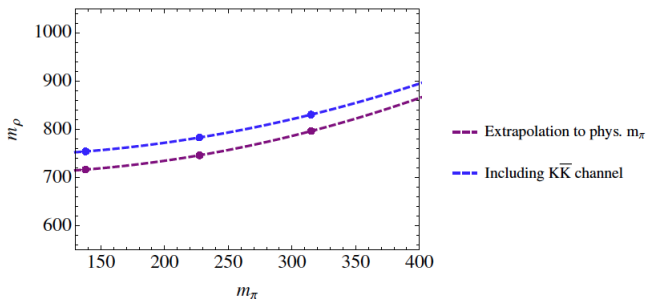


Figure : The  $K\bar{K}$  channel correction vs pion mass from a global fit for two pion mass.

$m_\pi$	$m_\rho$	$\Gamma_\rho$	$m'_\rho$	$\Gamma'_\rho$	$\chi^2/dof$
315	795.5(9)	36.5(3)	830.6(9)	51.4(3)	1.26
227	747.5(9)	77.4(6)	780.2(5)	97.8(3)	
138	719.7(1.6)	120.4(1.0)	754.6(0.5)	150.7(3)	

Global fit with  $U\chi PT$  for both pion mass. The definition of  $m_\rho$  is the value energy when the phase shift has  $\pi/2$ . The PDG value of  $\rho$  meson resonance parameter are  $m_\rho = 775.49$  MeV and  $\Gamma_\rho = 149.1$  MeV.

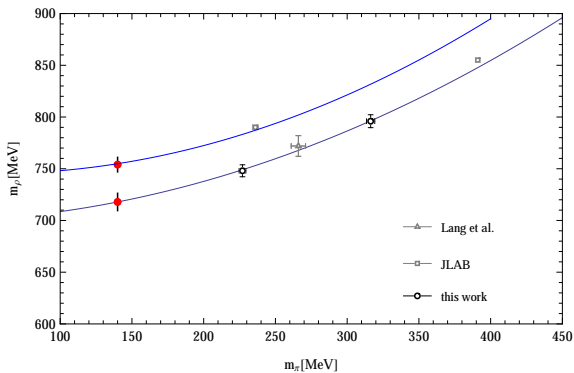


Figure : Result with  $K\bar{K}$  channel

# Conclusions

- We complete a precision study of  $\rho$  resonance with LapH smearing method and obtain the resonance parameters at  $m_\pi \approx 310$  MeV and  $m_\pi \approx 227$  MeV.
- For precise energy results, the Breit Wigner form only works in the resonance region. Modification to the BW is needed when applied to a wider energy region.
- The extrapolation of  $m_\rho$  to physical pion mass is smaller than  $m_\rho^{\text{phy}} = 775$  MeV in a  $N_f = 2$  situation, we believe that this comes from the absence of strange quark and the  $K\bar{K}$  channel which is supported by the unitary  $\chi$ PT study.



X. Feng, X. Li, and C. Liu, *Two particle states in an asymmetric box and the elastic scattering phases*, *Phys.Rev.* **D70** (2004) 014505, [hep-lat/0404001].



C. Morningstar, J. Bulava, J. Foley, K. J. Juge, D. Lenkner, et al., *Improved stochastic estimation of quark propagation with Laplacian Heaviside smearing in lattice QCD*, *Phys.Rev.* **D83** (2011) 114505, [arXiv:1104.3870].



F. Von Hippel and C. Quigg, *Centrifugal-barrier effects in resonance partial decay widths, shapes, and production amplitudes*, *Phys.Rev.* **D5** (1972) 624–638.



M. Luscher and U. Wolff, *How to calculate the elastic scattering matrix in two-dimensional quantum field theories by numerical simulation*, *Nucl.Phys.* **B339** (1990) 222–252.



P. Estabrooks and A. D. Martin,  *$\pi\pi$  Phase Shift Analysis Below the  $K$  anti- $K$  Threshold*, *Nucl.Phys.* **B79** (1974) 301.

# Symmetries on the lattice

The  $SO(3)$  symmetry group reduce to discrete subgroup  $O_h$  or  $D_{4h}$

**Table :** Resolution of  $2J + 1$  spherical harmonics into the irreducible representations of  $O_h$  and  $D_{4h}$

$J$	$O_h$	$D_{4h}$
0	$A_1^+$	$A_1^+$
1	$F_1^-$	$A_2^- \oplus E^-$
2	$E^+ \oplus F_2^+$	$A_1^+ \oplus B_1^+ \oplus B_2^+ \oplus E^+$
3	$A_2^- \oplus F_1^- \oplus F_2^-$	$A_2^- \oplus B_1^- \oplus B_2^- \oplus 2E^-$
4	$A_1^+ \oplus E^+ \oplus F_1^+ \oplus F_2^+$	$2A_1^+ \oplus A_2^+ \oplus B_1^+ \oplus B_2^+ \oplus 2E^+$

Assume that the energy contribution from angular momenta  $l \geq 3$  is negligible. For example, if we study the p-wave ( $l = 1$ ) scattering channel, we should construct the interpolating field in  $F_1^-$  in the  $O_h$  group,  $A_2^-$  and  $E^-$  representations in  $D_{4h}$  group.



## Variational method [4]

Variational method is used to extract energy of the excited states.

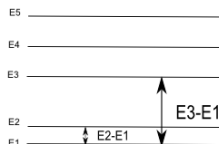
Construct correlation matrix in the interpolator basis

$$C(t)_{ij} = \langle \mathcal{O}_i(t) \mathcal{O}_j^\dagger(0) \rangle; i, j = 1, 2, \dots, \text{number of operators} \quad (24)$$

The eigenvalues of the correlation matrix are

$$\lambda^{(n)}(t, t_0) \propto e^{-E_n t} (1 + \mathcal{O}(e^{-\Delta E_n t})), n = 1, 2, \dots, \text{number of operators} \quad (25)$$

where  $\Delta E_n = E_{\text{Number of operators} + 1} - E_n$ .



Larger energy gap makes the high lying energy decay faster and effective mass plateau appear in an earlier time slice.

## Appendix-B: LapH smearing

Benefit from LapH smearing:

- Keep low frequency mode up to  $\Lambda$  cutoff to compute the all to all propagators,  $u(x) \longrightarrow u(y)$ . The number of propagators  $M^{-1}(t_f, t_i)$  need to be computed reduce from  $6.34 \times 10^{13}$  in position space to  $3.7 \times 10^8$  in momentum space for the  $24^3 48$  ensemble.
- The effective mass reach a plateau in an earlier time slice.

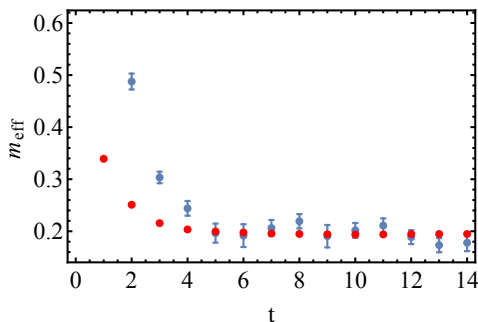


Figure : pion effective mass with (red) and without LapH smearing (blue)

## Appendix-C: Fitting phase-shift

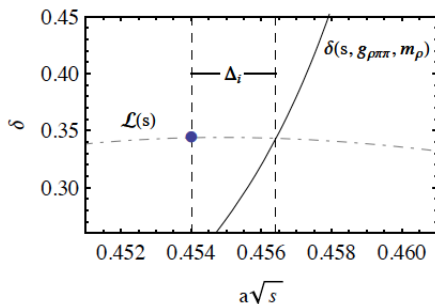


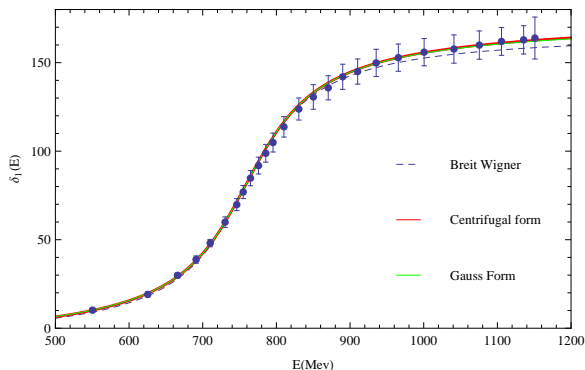
Figure :  $\chi^2$  fitting for the phase shift data to Breit Wigner form

$$\chi^2 = \Delta^T \text{COV}^{-1} \Delta \quad (26)$$

where

$$\Delta_i = \sqrt{s_i^{\text{curve}}} - \sqrt{s_i^{\text{data}}} \quad (27)$$

## Appendix-D: Experiment data [5]



$$\Gamma_{BW}(E) = \frac{g^2}{6\pi} \frac{p^3}{E^2}$$

$$\Gamma_{CF}(E) = \frac{g^2}{6\pi} \frac{p^3}{E^2} \frac{1 + (p_R R)^2}{1 + (p R)^2}$$

$$\Gamma_{GA}(E) = \frac{g^2}{6\pi} \frac{p^3}{E^2} \frac{e^{-p^2/6\beta^2}}{e^{-p_R^2/6\beta^2}}$$

Figure :  $\pi\pi$  phase shift below  $K\bar{K}$  threshold in experiment

[5] Estabrooks, P. and Martin, Alan D. Nucl.Phys. B79 (1974) 301

## K-matrix method

$$T^{-1} = V^{-1} - G = \frac{-3(f^2 - 8l_1 m_\pi^2 + 4l_2 W^2)}{2p^2} - \text{Re}G(W) + \frac{ip}{8\pi W} \quad (28)$$

For K-matrix method the  $\text{Re}G(W) = 0$ .

$$T = \frac{-8\pi W}{p \cot \delta p - ip} \quad (29)$$

$$l_1 = \frac{1}{8\pi^2} \left( -\frac{1}{2} \frac{m_\rho^2}{g_{\rho\pi\pi}^2} + f^2 \right) \quad (30)$$

$$l_2 = -\frac{1}{8g_{\rho\pi\pi}^2} \quad (31)$$